

Nanocluster Si sensitized Er luminescence: Excitation mechanisms and critical factors for population inversion

In Yong Kim, Kyung Joong Kim, and Jung H. Shin

Citation: *Appl. Phys. Lett.* **101**, 141907 (2012); doi: 10.1063/1.4757001

View online: <http://dx.doi.org/10.1063/1.4757001>

View Table of Contents: <http://apl.aip.org/resource/1/APPLAB/v101/i14>

Published by the [American Institute of Physics](http://www.aip.org).

Related Articles

Ultrabroadband terahertz conductivity of Si nanocrystal films

Appl. Phys. Lett. **101**, 211107 (2012)

Spectral patterns underlying polarization-enhanced diffractive interference are distinguishable by complex trigonometry

Appl. Phys. Lett. **101**, 183104 (2012)

Near-infrared enhanced carbon nanodots by thermally assisted growth

Appl. Phys. Lett. **101**, 163107 (2012)

Silicon nanoparticle-ZnS nanophosphors for ultraviolet-based white light emitting diode

J. Appl. Phys. **112**, 074313 (2012)

High energy-resolution electron energy-loss spectroscopy study on the near-infrared scattering mechanism of Cs_{0.33}WO₃ crystals and nanoparticles

J. Appl. Phys. **112**, 074308 (2012)

Additional information on *Appl. Phys. Lett.*

Journal Homepage: <http://apl.aip.org/>

Journal Information: http://apl.aip.org/about/about_the_journal

Top downloads: http://apl.aip.org/features/most_downloaded

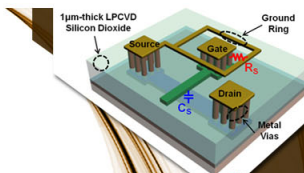
Information for Authors: <http://apl.aip.org/authors>

ADVERTISEMENT



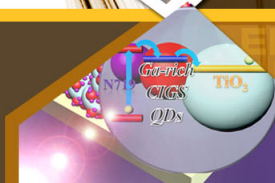
**EXPLORE WHAT'S
NEW IN APL**

SUBMIT YOUR PAPER NOW!



SURFACES AND INTERFACES

Focusing on physical, chemical, biological, structural, optical, magnetic and electrical properties of surfaces and interfaces, and more...



ENERGY CONVERSION AND STORAGE

Focusing on all aspects of static and dynamic energy conversion, energy storage, photovoltaics, solar fuels, batteries, capacitors, thermoelectrics, and more...

Nanocluster Si sensitized Er luminescence: Excitation mechanisms and critical factors for population inversion

In Yong Kim,¹ Kyung Joong Kim,² and Jung H. Shin^{1,3,a)}

¹Department of Physics, KAIST 335 Gwahak-ro, Yuseong-Gu, Daejeon 305-701, South Korea

²Division of Industrial Metrology, KRIS, 209 Gajeongno, Yuseong-gu, Daejeon 305-340, South Korea

³Graduate School of Nanoscience and Technology (WCU), KAIST 335 Gwahak-ro, Yuseong-Gu, Daejeon 305-701, South Korea

(Received 23 July 2012; accepted 18 September 2012; published online 4 October 2012)

Luminescence from Er³⁺ ions sensitized by nanocluster Si is investigated using finite-element, Monte-Carlo simulations. We find that we can reproduce and explain many conflicting results that have been reported using only a simple Förster-type interaction. In particular, we show that Er-Er energy migration plays a major role in Er³⁺ excitation such quantities such as excitation distance and sensitized fraction depend on optically active Er fraction and pumping power. Based on simulation results, we identify optically active fraction as the critical factor and suggest a multi-layered structure as being ideal for achieving population inversion. © 2012 American Institute of Physics. [<http://dx.doi.org/10.1063/1.4757001>]

Light emission from silicon has been the subject of intense research, both as a fundamental problem in semiconductor physics and as a practical application in the field of silicon photonics.¹ Of the many approaches, using a combination of nanocluster Si (nc-Si) and Er³⁺ together in a matrix²⁻⁴ has attracted a particular attention. In this case, nc-Si act as sensitizers that collect and transfer energy to the 4f shells of Er³⁺ ions with an effective excitation cross section that is both broad and orders of magnitude larger than the direct, optically resonant excitation cross-section of Er³⁺, while Er³⁺ ions in turn provide stable, intra-4f emission at 1.54 μm that is compatible with both SOI-based micro-photonics and long-distance telecom.⁵⁻⁷ By now, both broadband pumping using low-cost light sources^{8,9} and electrical excitation¹⁰ have been demonstrated, raising the possibility that nc-Si sensitized Er³⁺ can provide a low-cost 1.54 μm light source in a CMOS compatible platform.

Yet despite years of research, much of even basics of the sensitization process remain under dispute. For instance, many researchers have reported that the energy transfer from nc-Si to Er³⁺ decreases as $\exp[-x/x_0]$, with an “interaction distance” x_0 of less than 1 nm, suggesting a short-range, Dexter-type interaction.¹¹⁻¹³ In direct contrast, it was recently reported that nc-Si can excite Er³⁺ from as far as 7 nm away.¹⁴ Such a long-range interaction is incompatible with a Dexter-type interaction, but compatible with a Förster-type interaction that often plays a dominant role in energy transfer processes at the nanoscale.¹⁵ Indeed, Förster-type energy transfer among Er³⁺ ions has long been known to impact the Er³⁺ luminescence properties.¹⁶ Resolving this uncertainty is critical not only for the scientific understanding of the system, but also for its technological applications as well. If energy transfer is limited to sub-nm distances, then only a very low fraction of doped Er³⁺ would be sensitized such that population inversion would be impossible, while energy transfer across several nm would, in principle, enable population

inversion. Indeed, reported values of sensitized fraction ranges from as low as 3%¹⁷ to >50%.¹⁸

In this paper, we report on results of a finite-element, Monte-Carlo simulation of nc-Si sensitization of Er³⁺. By using Monte-Carlo simulation instead of rate equation, it is possible to vary the material structure and composition arbitrarily on sub-nm scale to investigate their effect. We find that a single, Förster-type interaction between nc-Si and Er³⁺, together with the well-known Er-Er energy migration, is sufficient to reproduce the wide range of conflicting results that have been reported. In fact, many disputed quantities such as apparent interaction distance and sensitized fraction are dependent on sample structure and other incidental experimental conditions. Based on simulations results, we identify the optically active fraction of Er as a critical factor that controls population inversion and suggest a multi-layered structure as being ideal for achieving population inversion.

For simulations, a cubic grid with a cell size of $0.2 \times 0.2 \times 0.2 \text{ nm}^3$, and a time step (Δt) of 1 ns was used. The volume simulated consisted of an area of $40 \text{ nm} \times 40 \text{ nm}$, with thicknesses as appropriate for each simulation. The grid size and time steps were confirmed to be small enough not to produce any significant artifacts. A cell can be empty, or singly occupied by either an nc-Si or an Er³⁺ ion. All nc-Si are assumed to be active: that is, they are all equally capable of transferring energy to nearby Er³⁺ ion. On the other hand, some Er ions are assumed to be inactive: that is, they can be excited by energy transfer, but immediately undergo non-radiative decay to the ground state. The system is then subjected to continuous illumination and allowed to evolve on its own according to the following simple rules: (i) only the nc-Si absorb pump photons; (ii) excited nc-Si can decay, transfer energy to Er³⁺, or do nothing; (iii) excited Er³⁺ ions can decay, transfer energy to nearby Er³⁺, or do nothing. The rate of nc-Si excitation, W , is given by $\sigma_{\text{abs}}\phi$, where σ_{abs} is the absorption cross-section of nc-Si, and ϕ is the photon flux. The decay rates of excited nc-Si and active Er³⁺ are given by $1/\tau$, where τ is their decay lifetimes. The nc-Si–

^{a)}E-mail: jhs@kaist.ac.kr.

Er^{3+} and $\text{Er}^{3+}\text{-Er}^{3+}$ transfer rates are both assumed to be a Förster-type interaction of the form $W = \frac{1}{\tau_x} \left(\frac{r_0}{r}\right)^6$, where τ_x is the lifetime of the excited donor, r_x is the critical transfer distance at which the energy transfer and spontaneous decay of the excited donor have equal probability, and r is the donor-acceptor distance.¹⁵ The probability that an energy transfer process occurs within a single time step during simulation is then given by $W\Delta t$. In all cases, an Er concentration of 10^{20} cm^{-3} and nc-Si concentration of 10^{19} cm^{-3} were used, and results of more than 10 simulations were averaged. An example of the material structure, the flow chart for the simulation and the values of the parameters used in simulations are summarized in Fig. 1 and Table I, respectively. We take the radiative lifetime of nc-Si ($\tau_{nc\text{-Si}}$) and Er ($\tau_{Er\text{-rad}}$) to be $40 \mu\text{s}$ and 10 ms , respectively. On the other hand, the actual decay time of Er^{3+} ($\tau_{Er\text{-decay}}$) is taken to be 1 ms , which is the value typically observed from nc-Si sensitized Er^{3+} systems, in order to take into account the possibility of non-radiative decay paths. The critical transfer distance for $\text{Er}^{3+}\text{-Er}^{3+}$ energy migration (r_{mig}) and cooperative upconversion (r_{CU}) of Er are taken to be 1.8 and 1.0 nm , respectively.¹⁹ The critical transfer distance for nc-Si- Er^{3+} energy transfer is taken to be $r_{tr} = 3 \text{ nm}$, in accordance with Ref. 14.

Several points are worthy of note. By placing an nc-Si in a single cell, we are assuming that nc-Si are point-particles. This is based on reports that suggest that Er^{3+} sensitization is dominated by small, defect-like centers, possibly related to nc-Si, not by entire nc-Si.^{12,20} However, we will use the word “nc-Si” to mean sensitizing centers to avoid confusion. We allow energy transfer to both excited and ground state Er^{3+} , thus automatically including important non-linear effects such as excited state absorption, energy migration, and cooperative upconversion. For instance, an energy transfer from an excited Er^{3+} to an Er^{3+} in the ground state represents energy migration, while an energy transfer from an excited Er^{3+} to another excited Er^{3+} represents cooperative upconversion. On the other hand, we neglect back-transfer of energy from an excited Er^{3+} to a nc-Si as well as the free carrier absorption, since such processes are minimized in low-temperature annealed

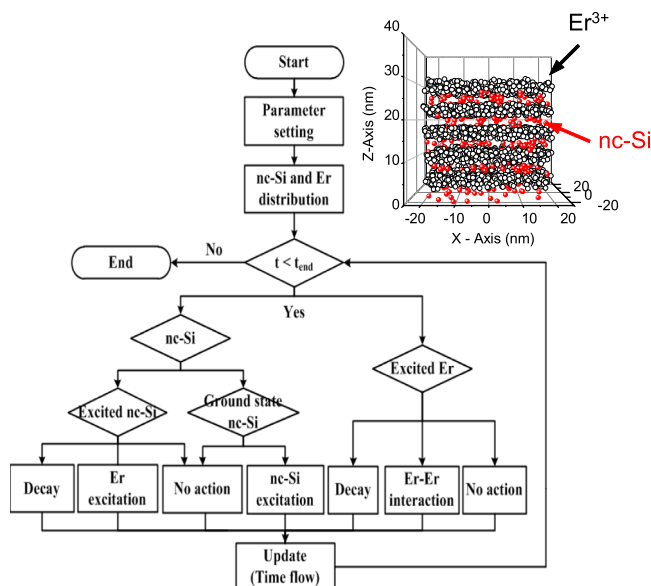


FIG. 1. The flow chart of simulations and an example of the structures.

TABLE I. Physical parameters used in simulation.

Parameter	Value
$\tau_{nc\text{-Si}}$	$40 \mu\text{s}$
$\tau_{Er\text{-decay}}$	1 ms
$\tau_{Er\text{-rad}}$	10 ms
r_{tr}	3 nm
r_{mig}	1.8 nm
r_{cu}	1.0 nm
σ_{abs}	10^{-15} cm^2

films that maximize formation of such sensitizing centers,²¹ and some of their effects can be accounted for by adjusting other parameters such as the optically active fraction. Still, the simulated structure should be understood to be an idealized system whose results represent the upper limit of experimentally achievable values. In all cases, we keep track of the number of excited particles, which we take to be proportional to experimentally observable photoluminescence (PL) intensity.

We first investigate the controversy regarding the nc-Si- Er^{3+} interaction distance using a double-layer structure with a 2 nm thick nc-Si layer and an Er-doped layer. All Er ions are assumed to be active and ϕ is $10^{19} \text{ photons/cm}^2 \text{ s}$. Figure 2(a) shows the effect of increasing the distance between the nc-Si layer and an Er-doped layer of a fixed thickness, as discussed in Ref. 14. Figure 2(b) shows the effect of increasing the thickness of the Er-doped layer that is in contact with a nc-Si layer, as discussed in Ref. 11 and 13. In the first case, the decrease in the Er^{3+} PL intensity with distance from the nc-Si layer is well-described by an exponential of the form $\exp[-x/x_0]$, where x is the distance between the Er^{3+} layer and the nc-Si layer, with an apparent “interaction distance” x_0 of 3.4 nm , in good agreement with the value of 3.8 nm reported in Ref. 14. In the second case, the decrease in the nc-Si PL intensity with increasing Er^{3+} layer thickness is again well-described by an exponential of the form $\exp[-x/x_0]$, where x is the Er^{3+} layer thickness, but this time with an apparent “interaction

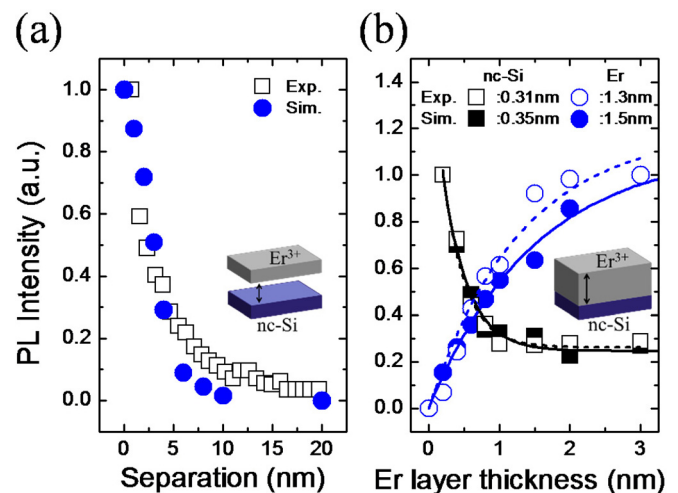


FIG. 2. (a) Effect of increasing the nc-Si-Er distance on the sensitized Er. The open symbols are experimental data from Ref. 14, and the closed symbols are the results of simulation. (b) Effect of increasing the Er layer thickness. The open symbols are experimental data from Ref. 13, and the closed symbols are the results of simulation. Squares and circles are results of nc-Si and Er, respectively. The dashed lines and solid lines are exponential fits of experimental and simulations results, respectively.

distance” of only 0.35 nm, in agreement with previous reports of very short “interaction distance.”^{11,13}

In addition, Fig. 2(b) also reproduces another important feature in the experimental results: the Er^{3+} PL continues to increase with increasing Er^{3+} layer thickness even after the nc-Si PL has ceased to decrease, suggesting a much larger apparent “interaction distance” of 1.5 nm.¹³ This disparity points out an important effect that is often overlooked: the Er-Er energy migration. Figure 3(a) shows typical simulation results of a double-layer structure (similar to that in Fig. 2(b)) under identical conditions except for Er-Er energy migration. We find that in both cases, the number of excited Er^{3+} ions decreases exponential-like with the distance from the nc-Si layer. Without Er-Er energy migration, the typical decay distance is only 1.1 nm. However, when Er-Er energy migration is allowed, it increases to 2.6 nm, resulting in a nearly two-fold increase of the total number of excited Er^{3+} ions, since Er^{3+} ions that are far away from the nc-Si layer can be excited via Er^{3+} ions that are closer. As these donor Er^{3+} ions can then be excited again via nc-Si, increasing the photon flux increases the apparent “interaction distance” of Er^{3+} , as is shown in Fig. 3(b), again in agreement with experimental results reported in Ref. 13.

It should be stressed here that these reproductions of a wide range of reported experimental results, including the conflicting reports of short- and long-range interactions are all based on the single set of simulation parameters given in Table I. Thus, they show that the observed exponential-like behavior of the form $\exp[-x/x_0]$, with an apparent “interaction distance” of x_0 , does not necessarily rule out a Förster-type interaction. Rather, integrating the dipole interaction across many distances and directions results in distance dependence that looks like an exponential in a planar geometry.¹⁴ Similarly, the short nm-scale “interaction distance” does not necessarily imply a similarly short-ranged Dexter-type energy transfer mechanism. Rather, it simply reflects the fact that a nc-Si interacts mostly strongly with the nearest Er^{3+} ion which, given typical Er concentrations used in experiments, is likely to lie within the first nm-thin

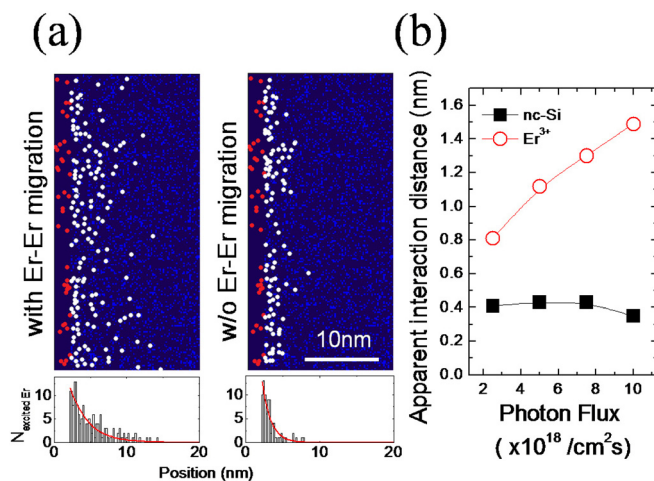


FIG. 3. (a) Typical simulation results of a double layer structure with and without Er-Er energy migration. White points and red points are excited Er and nc-Si, respectively. Histograms show the number of excited Er^{3+} ions, and the red line is an exponential fit. (b) The effect of increasing the photon flux upon the apparent interaction distance of nc-Si and Er^{3+} .

layer next to it. In fact, the idea of an “interaction distance” that is characteristic of a particular mechanism seems suspect, as simple changes in sample geometry, composition, or pump conditions can greatly affect its value.

So far, we have assumed that all of doped Er^{3+} ions are optically active. In such a case, energy migration can greatly increase the number of Er^{3+} ions that can be sensitized via nc-Si, as shown above. However, in typical thin films created by deposition, the presence of defects can lead to optical deactivation of a significant fraction of Er^{3+} ion.¹⁷ In such a case, the Er-Er energy migration can lead to concentration quenching where a single optically inactive Er^{3+} acts as a non-radiative decay path for many nearby Er^{3+} ions. This is demonstrated in Fig. 4(a) that show the simulated decay traces of Er^{3+} luminescence. We find that the presence of optically inactive Er^{3+} reduces the Er^{3+} luminescence decay time and changes the decay trace from a single-exponential to a stretched exponential of the form $\exp\{-(t/t_0)^\beta\}$. Actually, such a stretched exponential decay is often observed from nc-Si sensitized Er^{3+} .²² While many different physical mechanisms can lead to such a stretched exponential decay,²³ our results suggest that it can also be an indication of presence of optically inactive Er^{3+} . Unfortunately, such optically inactive Er^{3+} does far more damage than simply reducing the luminescence efficiency. As shown in the

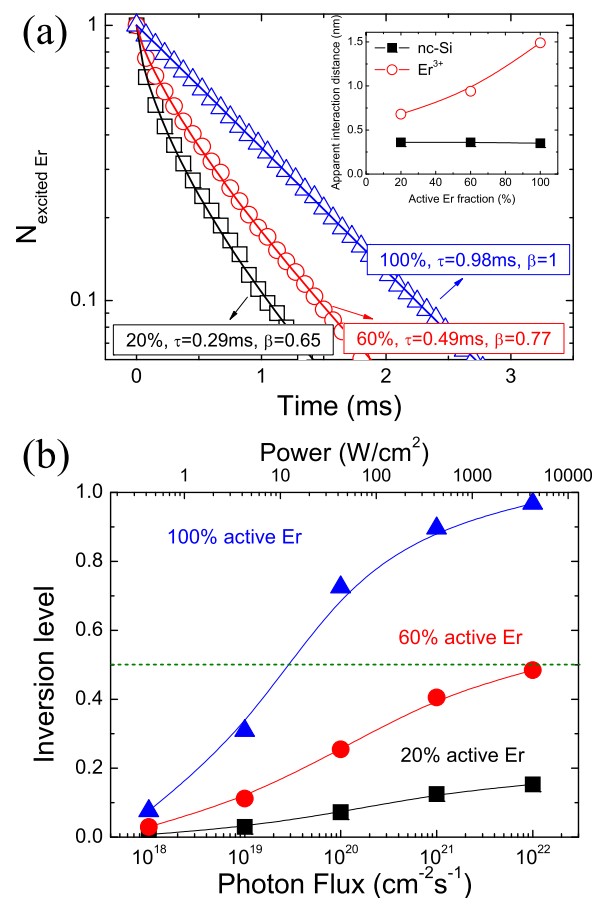


FIG. 4. (a) Effect of optically inactive Er^{3+} on the Er^{3+} luminescence decay trace. The symbols are simulation results, and the lines are fit to the stretched exponential of the form $\exp\{-(t/t_0)^\beta\}$. The inset show the effect of optically inactive Er^{3+} on the apparent nc-Si/Er interaction distance. (b) The effect of optically inactive Er^{3+} on population inversion. In this case, a homogeneous structure with random location of nc-Si and Er in 3D is assumed.

inset of Fig. 4(a), reducing the fraction of optically active Er^{3+} significantly reduces the distance across which an Er^{3+} ion can be excited by a layer of nc-Si as well. As a result, achieving population inversion via nc-Si sensitization is seriously compromised. This is shown in Fig. 4(b), which shows the simulated Er^{3+} inversion level of a homogeneous thin film in which both nc-Si and Er are randomly distributed in 3D. All simulation parameters were the same except for the active Er^{3+} fraction. We find that reducing the optically active fraction from 100% to 60% does not simply scale the inversion level by 60%. At a pump power of 2.7×10^{19} photons/cm² s (~ 1 W/cm² at 470 nm) that would result in 50% inversion of a film with 100% optically active Er, the film with 60% optically active Er reaches an inversion level of only 17%. In fact, it does not achieve population inversion even under an unrealistically high photon flux of 10^{22} photons/cm² s (~ 4200 W/cm² at 470 nm).

Above results suggest that in achieving population inversion of Er^{3+} , the fraction of optically active Er^{3+} is the critical even with nc-Si sensitization. Practically, this would indicate that in preparing samples, optimizing the Er^{3+} decay trace for long luminescence lifetimes and single-exponential decay should take the first priority. Recently, we have reported that, by using nitrides instead of oxides, such a material with near 100% optically active fraction can be achieved while maintaining significant sensitization.²⁴ Thus, we now investigate how we may optimize the material structure for population inversion. For this purpose, we compare the homogeneous structure used in Fig. 4(b) with a multilayer structure in which nc-Si and Er^{3+} are separated into 2 nm-thick nc-Si layers and 0.2 nm-thick Er-doped layers. Local densities of Er and nc-Si in multilayers are the same as those in the homogeneous structure. Figure 5 shows the inversion levels of two structures as a function of photon flux. We find that population inversion in the multilayer structure can be achieved with photon flux of only 2.4×10^{18} photons/cm² s, one order of magnitude lower than the homogeneous structure. Indeed, with a multilayered structure, population inversion is possible even with an optically active Er^{3+} fraction of only 60%, since a multilayer structure mini-

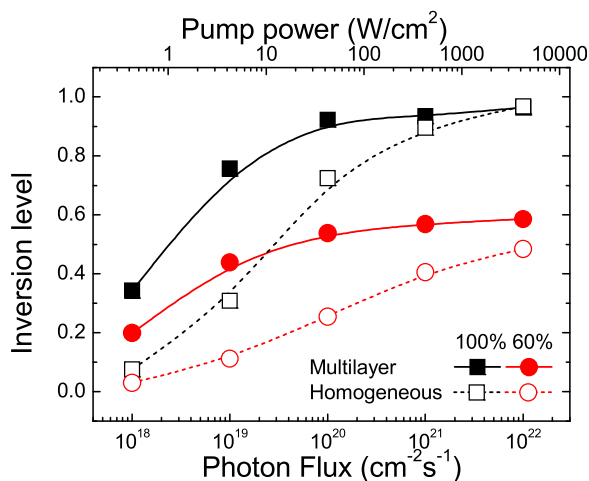


FIG. 5. Simulated Er^{3+} population inversion levels of a homogeneous thin film with random, 3D distribution of both nc-Si and Er, and a multilayered thin film with 2 nm-thick nc-Si layers and 0.2 nm-thick Er-doped layers. Local densities of Er and nc-Si in multilayers are the same in both cases.

mizes concentration quenching while maximizing the nc-Si and Er interaction. These results are consistent with experimental reports on the advantages of such multilayered structure^{18,25} and suggests that for nc-Si sensitized Er emission, nano-scale engineering of the structure to ensure close contact of all of the doped Er^{3+} with nc-Si should be performed.

In conclusion, we have investigated the Er sensitization mechanism and prospect of population inversion with Monte-Carlo simulation. We find that a simple Förster-type interaction can explain much of the conflicting report. In particular, we show that Er-Er energy migration has a significant effect upon the overall sensitization process, and that as a consequence, quantities such as apparent interaction distance and sensitized fraction are condition-dependent without a fixed value, while the optically active fraction of Er becomes the critical factor for population inversion. Based on simulation results, we suggest a multilayered structure as being ideal for achieving population inversion.

This work was supported in part by the National Research Foundation of Korea (NRF) grant funded by the Korea government (MEST) (Grant No. 2011-0029868, Basic Science Research Program: Grant No. 2009-0087691). J. H. Shin acknowledges support by WCU (World Class University) program, Grant No. R31-2008-000-10071-0.

¹L. Pavesi, *J. Phys.: Condens. Matter* **15**, R1169 (2003).

²A. J. Kenyon, P. F. Trwoga, M. Federighi, and C. W. Pitt, *J. Phys.: Condens. Matter* **6**, L319 (1994).

³M. Fujii, M. Yoshida, Y. Kanzawa, S. Hayashi, and K. Yamamoto, *Appl. Phys. Lett.* **71**, 1198 (1997).

⁴J. H. Shin, M.-J. Kim, S.-Y. Seo, and C. Lee, *Appl. Phys. Lett.* **72**, 1092 (1998).

⁵P. G. Kik, M. L. Brongersma, and A. Polman, *Appl. Phys. Lett.* **76**, 2325 (2000).

⁶D. Pacifici, G. Franzò, F. Priolo, F. Iacona, and L. Dal Negro, *Phys. Rev. B* **67**, 245301 (2003).

⁷F. Gourbilleau, M. Levalois, C. Dufour, J. Vicens, and R. Rizk, *J. Appl. Phys.* **95**, 3717 (2004).

⁸A. J. Kenyon, C. E. Chryssou, C. W. Pitt, T. Shimizu-Iwayama, D. E. Hole, N. Sharma, and C. J. Humphreys, *Mater. Sci. Eng., B* **81**, 19 (2001).

⁹J. Lee, J. H. Shin, and N. Park, *J. Lightwave Technol.* **23**, 19 (2005).

¹⁰O. Jambois, F. Gourbilleau, A. J. Kenyon, J. Montserrat, R. Rizk, and B. Garrido, *Opt. Express* **18**, 2230 (2010).

¹¹J.-H. Jhe, J. H. Shin, K. J. Kim, and D.W. Moon, *Appl. Phys. Lett.* **82**, 4489 (2003).

¹²A. Pitanti, D. Navarro-Urrios, N. Prtljaga, N. Daldosso, F. Gourbilleau, R. Rizk, B. Garrido, and L. Pavesi, *J. Appl. Phys.* **108**, 053518 (2010).

¹³I. Y. Kim, J. H. Shin, and K. J. Kim, *Appl. Phys. Lett.* **95**, 221101 (2009).

¹⁴K. Choy, F. Lenz, X. X. Liang, F. Marsiglio, and A. Meldrum, *Appl. Phys. Lett.* **93**, 261109 (2008).

¹⁵T. Förster, *Discuss. Faraday Soc.* **27**, 7 (1959).

¹⁶M. J. A. de Dood, J. Knoester, A. Tip, and A. Polman, *Phys. Rev. B* **71**, 115102 (2005).

¹⁷S. Minissale, T. Gregorkiewicz, M. Forcales, and R. G. Elliman, *Appl. Phys. Lett.* **89**, 171908 (2006).

¹⁸S. Núñez-Sánchez, P. M. Roque, R. Serna, and A. K. Petford-Long, *Appl. Phys. Lett.* **98**, 151109 (2011).

¹⁹J. L. Philipsen and A. Bjarklev, *IEEE J. Quantum Electron.* **33**, 845 (1997).

²⁰O. Savchyn, F. R. Ruhge, P. G. Kik, R. M. Todi, K. R. Coffey, H. Nukala, and H. Heinrich, *Phys. Rev. B* **76**, 195419 (2007).

²¹S.-Y. Seo and J. H. Shin, *Appl. Phys. Lett.* **75**, 4070 (1999).

²²G. Franzò, E. Pecora, F. Priolo, and F. Iacona, *Appl. Phys. Lett.* **90**, 183102 (2007).

²³O. Savchyn, R. M. Todi, K. R. Coffey, and P. G. Kik, *Appl. Phys. Lett.* **93**, 233120 (2008).

²⁴J. S. Chang, I. Y. Kim, G. Y. Sung, and J. H. Shin, *Opt. Express* **19**, 8406 (2011)

²⁵I. Y. Kim, K. J. Kim, and J. H. Shin, *J. Appl. Phys.* **108**, 073101 (2010).